JOURNAL OF MATERIALS SCIENCE 29 (1994) 3510–3516

Electrostatic charge distribution in the dielectric layer of alumina electrostatic chuck

T. WATANABE, T. KITABAYASHI, C. NAKAYAMA
R and D Division, T Ltd. 2-8-1, Honson, Chigasaki-shi, Kanagawa 253, Japan

Electrostatic charge and its distribution in the dielectric layer of TiO_2- and Cr_2O_3-added alumina electrostatic chucks has been studied. The electrostatic potential was evaluated at various applied voltages by an electrostatic potential meter and it demonstrated the existence of charges with opposite polarities. Direct SEM observation and toner development of the charged ceramic surface was carried out to clarify the charge distribution. The charge contrast was not uniform on the ceramic microstructure and the charge was distributed in the form of grains. Taking into consideration these results, the relationship between electrostatic charge distribution and ceramic microstructure is discussed.

1. Introduction

An alumina electrostatic chuck doped with TiO_2 exhibits a large adhesion force, compared with a polymer electrostatic chuck or the common ceramic electrostatic chuck [1]. Recent investigations have clarified that the electrostatic force depends on the space charge distribution on the dielectric layer, and the distribution is affected by the surface resistance and bulk resistance of the dielectric layer [2]. Therefore, many factors, such as the measuring atmosphere or surface contaminations, affect electrostatic force. Besides instability of the electrostatic force, residual electrostatic force is another problem in the application of the chuck in semiconductor manufacturing apparatus, because throughput of the apparatus is dependent on the time required to unload the wafer [3]. In order to apply the electrostatic chuck to such practical uses, it is necessary to optimize the charge distribution in the dielectric layer to control the electrostatic force.

Space charge in various polymer materials was investigated by Thermal stimulated current (TSC) [4], Thermal pulse current (TPC) [5], or absorption current [6, 7] methods. It is known that a homocharge, i.e. a charge with the same polarity as that of the facing electrode, is observed in electret materials, as well as a heterocharge, i.e. a charge with an opposite polarity to that of the electrode. In ferroelectric ceramics such as Pb(Zr, Ti)O_3 (PZT) or (Pb, La) (Zr, Ti)O_3 (PLZT), polarization properties were affected by the space charge [8, 9], and their distribution in the thickness of the dielectric layer was evaluated by pressure wave [10], Laser intensity modulation method (LIMM) [11, 12] or absorption current [13] methods.

In ZnO and other semiconductor materials, the interface state near the grainboundary was evaluated by the capacitance vs voltage (CV) method [14], deep level transient spectroscopy (DLTS) [15] and isothermal capacitance transient spectroscopy (ICTS) [16]. In many cases, the space charge is considered to be located on the grain boundaries or interfaces because of the presence of lattice vacancies and impurities.

Although many investigations have been made on the space charge and its microstructural distribution, its detailed location in material microstructure is, as yet, unsubstantiated.

In this paper, detailed charge distribution was evaluated via direct observation of the charge location by SEM. The charge potential was also measured by an electrostatic potential meter to examine the decay characteristics of the space charge. In accordance with the measured results, the effects of ceramic microstructure on the space charge and its electrostatic force are discussed.

2. Experimental procedure

2.1. Materials and fabrication of samples

The electrostatic chuck samples used in this research were 89% alumina ceramics containing 1.3 wt % TiO_2, 3.5 wt % Cr_2O_3, 5.0 wt % SiO_2, 1.2 wt % CaO and 1.1 wt % MgO. The fabrication procedure of the sample has previously been described in detail earlier, so that only the essentials of the procedure will be represented here.

The sample, metallized with tungsten as an inner electrode, was fabricated by the conventional integrated circuit (IC) package manufacturing procedure. Sintering was carried out in $N_2 + H_2 + H_2O$ atmosphere at 1580 °C for 2 h. The size of the sintered samples was 50 mm × 50 mm × 2 mm. The dielectric layer of the chuck was polished to 300 μm with diamond pastes. The average roughness of the samples, R_a, was 0.4 μm and the flatness was less than 3 μm.

2.2. Electrostatic potential measurement

Decay of the electrostatic charge accumulated in the ceramic chuck was evaluated by electrostatic potential measurements. The evaluation procedure is shown in Fig. 1. First, voltage is applied between the electrostatic chuck and metal electrode to obtain charge

0022–2461

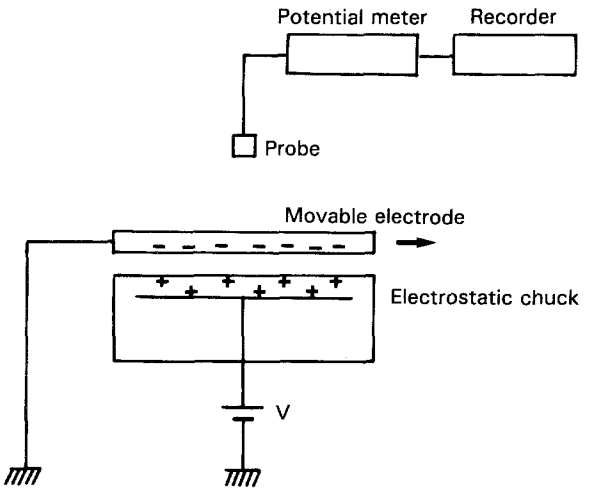

Figure 1 Schematic diagram of experimental arrangement for electrostatic potential measurement.

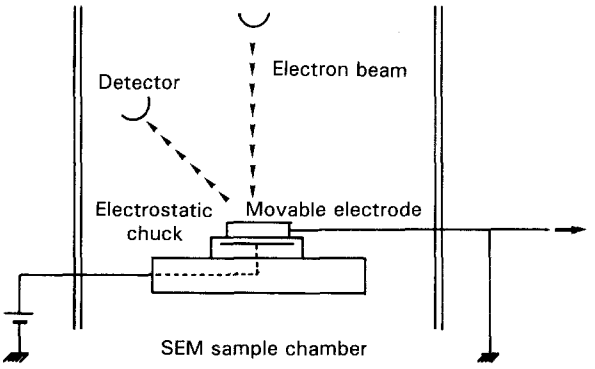

Figure 2 Schematic diagram of experimental arrangement for SEM observation of electrostatic charge distribution.

accumulation in the dielectric layer. At this stage, the electrostatic potential meter above the metal electrode detects no potential. Secondly, the metal electrode is removed to expose the charged surface. The potential meter begins to detect the electrostatic potential created by the space charge on and after removal of the electrode.

According to the above procedure, the decay of the accumulated charge is evaluated. The measurements were conducted in a vacuum chamber at 0.001 torr. A vibrating electrode potential meter (Trek Model 344, feedback type) was used for the measurements.

2.3. Microstructural observation

Microstructural observation and composition analysis were carried out by means of SEM using a dispersion-type characteristic X-ray analyser (Shimazu EPMA 8705 H III). The surface of the examined specimen was polished with diamond pastes and evaporation-coated with gold. Phase identification was carried out via X-ray (CuK_α) diffraction.

2.4. Observation of charge distribution

2.4.1. Toner development method

Charged substances can be developed with a toner consisting of charged particles. In order to observe the fine microstructure of charging, it is necessary to use fine particles as the developer. A liquid toner is suitable for this use because it has fine particles of about 0.1 μm diameter [17]. Therefore, we used a liquid toner (Ricoh PC-type toner 1000) consisting of negatively charged particles and a carrier liquid. The negatively charged toner particles concentrate on the positively charged portion on the ceramics, giving a positive charge distribution image.

The sample preparation procedure is as follows: a brass plate (30 mm diameter and 4 mm thick) was held on the electrostatic chuck by applying voltage. Then a drop of liquid toner was deposited on the electrostatic chuck immediately after removal of the metal plate. The deposited sample was dried for 1 h at 110 °C in an oven. Observation of the toner particle distribution was carried out by means of SEM (Hitachi S-800).

2.5. Observation of charge distribution

2.5.1. Direct observation by means of SEM

When conventional SEM observations of ceramic materials such as alumina ceramics is carried out, it is necessary to coat the sample with a thin conductive metal layer to prevent charging by the electron beam. However, in this experiment, it is necessary to observe the sample without using a conductive coating because the coating greatly affects the charge distribution on the ceramics. The degree of charging by the electron beam depends on both the surface resistivity and the beam acceleration voltage. We examined various acceleration voltages and clarified that a voltage below 1.5 kV prevents charging up by the electron beam, giving good microstructural photographs. Therefore, the following SEM observation of charged ceramics was conducted at an acceleration voltage of 1.5 kV.

The charge distribution observation was carried out using the following procedure, shown in Fig. 2. The ground brass plate (the same as that used in Section 2.4.1) is held on the electrostatic chuck in the SEM specimen chamber. The SEM used was a Hitachi S-800. The brass plate was connected to a wire which was drawn out of the specimen chamber. A negative or positive voltage was applied to the inner electrode of the chuck and SEM observation was conducted immediately after removal of the brass plate by pulling the wire.

3. Results and discussion

3.1. Electrostatic potential measurements

Fig. 3a shows the results of electrostatic potential measurements when the applied voltage is + 100 V. The potential, σ, decreases gradually with time and the maximum potential value, $\sigma(t = 0)$, increases with the duration of applied voltage. However, potential decay in the case of + 500 V is different from that of + 100 V, as shown in Fig. 3b. When the voltage application duration is below 30 s, the decay profile is similar to that at + 100 V. However, when the voltage application duration is longer than 30 s, a reverse

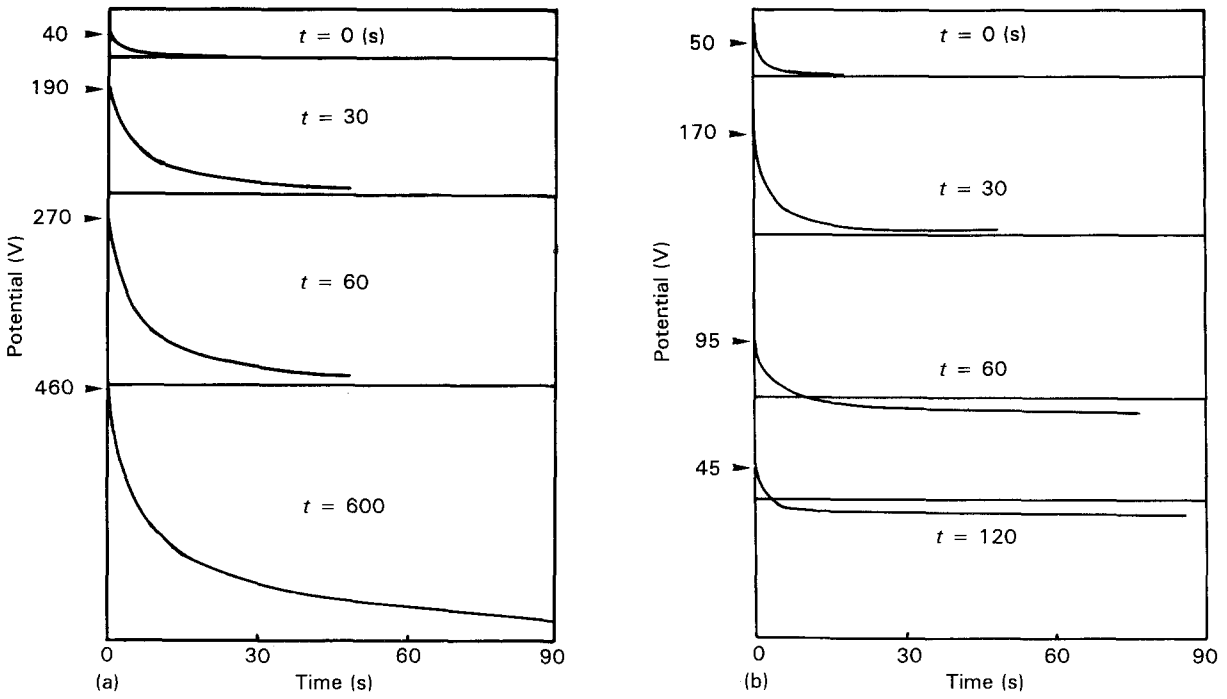

Figure 3 Electrostatic potential of a charged ceramic surface. The potential decay curve is represented for various voltage application durations. (a) Applied voltage 100 V, (b) applied voltage 500 V.

potential appears. At first, the potential decreases to zero and then the potential polarity switches. The reverse potential increases gradually and finally returns to zero. The reverse potential suggests the existence of a homocharge, a charge with the same polarity as that of the metal electrode. Homocharge is a charge injected from the electrode into the dielectric layer by corona discharging, contact current or other processes, and it lasts longer than the heterocharge, a charge with an opposite polarity to the electrode.

As shown in Fig. 3a, no homocharge appears in the ceramic layer when the applied voltage is low. This is reasonable if corona discharging causes the homocharge, because no discharge occurs below Paschen's discharging voltage (about 330 V in air).

3.2. Microstructural observation

Fig. 4a shows scanning electron micrographs of the fabricated Al_2O_3 ceramics. Angular alumina grains and the secondary phase are observed. The average grain size of alumina is about 5 μm and pore sizes range from 5–10 μm. Fig. 4b–d and f show EPMA image of aluminium, silicon, oxygen, titanium and chromium. The microstructure is composed of alumina grains containing Cr_2O_3 and a silicon-rich phase, but their distribution does not correspond to that of SiO_2. Powder X-ray diffraction study shows rutile present in the sintered body; therefore, most of the added TiO_2 distributed should be rutile.

3.3. Observation of charge distribution

3.3.1. Toner development method

Fig. 5a and b show SEM images of the negatively charged toner distribution on the ceramics when a positive voltage is applied. Most of the toner particles are observed to adhere circumferentially on the alumina grains and few of them are on the silicon-rich phase. Furthermore, many of the toner particles are on the grain boundaries between the alumina grains (arrows 1, 2) and on the interface between the alumina grains and silicon-rich phase (arrows 3, 4).

3.3.2. Direct observation by means of SEM

In order to clarify the space charge distribution in the ceramics, direct observation via SEM was carried out. Fig. 6a–d show serial charge contrasts on the ceramics after removal of the metal plate. The applied voltage is 100 V. The contrast lasts more than 600 s and decreases gradually with time. The contrast decay agrees well with the electrostatic potential decay shown in Fig. 3a. Fig. 6d shows an enlarged image of the contrast in Fig. 6b (square). Granular contrast of about 5 μm is observed in the image.

A series of photographs when the applied voltage is 500 V is shown in Fig. 6e–h. The contrast lasts more than 600 s and the decay is similar to that at 100 V. However, the granular contrast in the enlarged image of the photographs is not as clear as that at 100 V.

According to the electrostatic potential measurements shown in Fig. 3b, the space charge caused by 500 V application includes homocharge in addition to heterocharge. The indistinct contrast shown in Fig. 7 is attributed to the complicated electric field caused by the positive and negative charges.

Fig. 7 shows another example of a photograph of heterocharge granular contrast. The image was taken 30 s after removing metal plate. The granular contrast is distributed almost uniformly on the contact area; however, there is a minute change in contact which may be due to the contact condition.

Fig. 8 shows a photograph of such granular con-

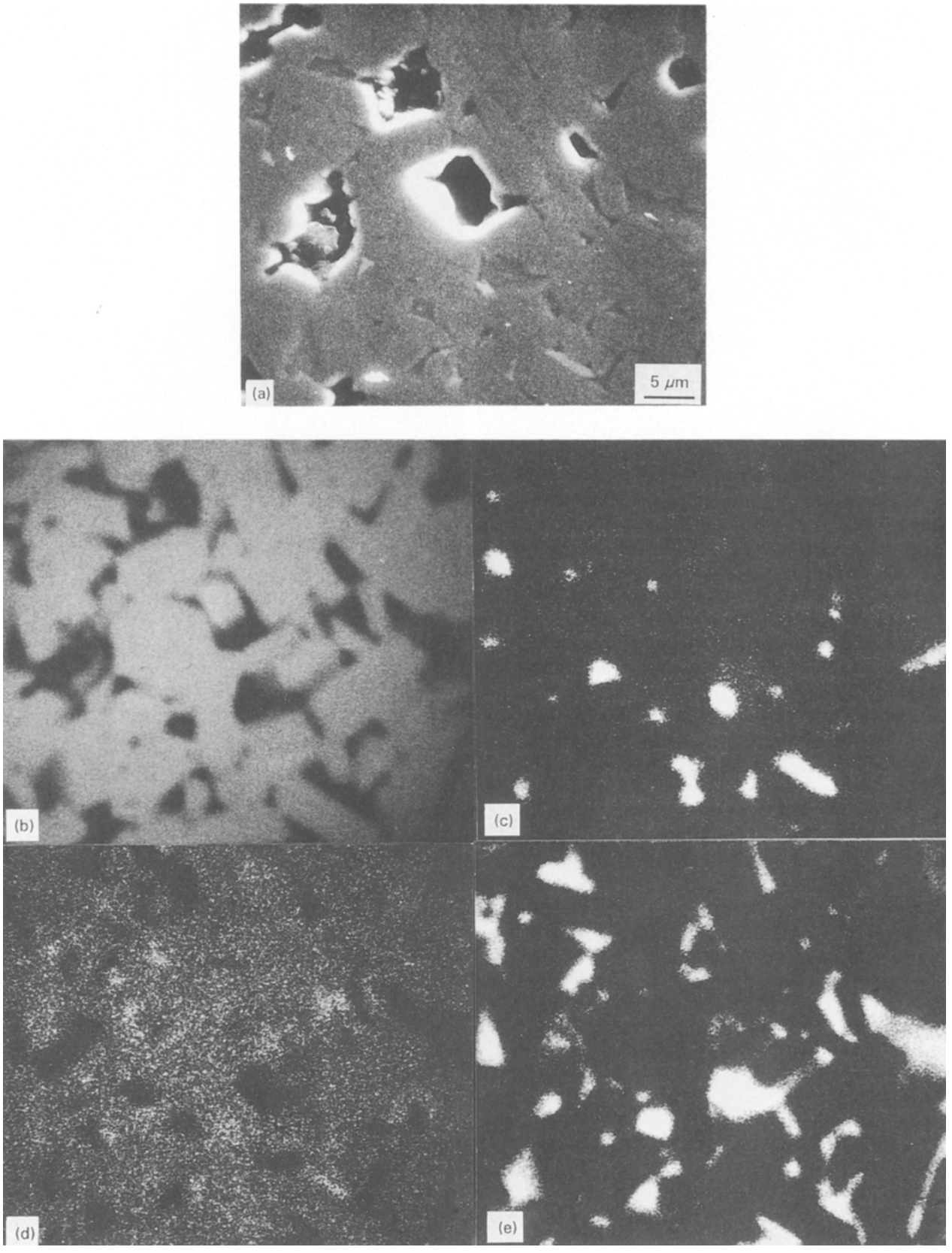

Figure 4 Scanning electron micrographs and EPMA images of cross-sections of Cr_2O_3- and TiO_2- added alumina. (a) SEM, (b) X-ray image of aluminium, (c) X-ray image of titanium, (d) X-ray image of chromium, (e) X-ray image of silicon.

trast and its corresponding microstructural SEM image. The latter was taken without voltage application to the inner electrode of the sample. In order to show accurately the location of charge contrast, an SEM field including adhered metal particles is represented in the figure.

In Fig. 8, contrasts A and B correspond to the area near the silicon-rich phases. According to the previous toner development experiment, the silicon-rich phase does not have a long-lasting charge; therefore, it is assumed that these charges are located on the interface between the alumina grains and the silicon-rich

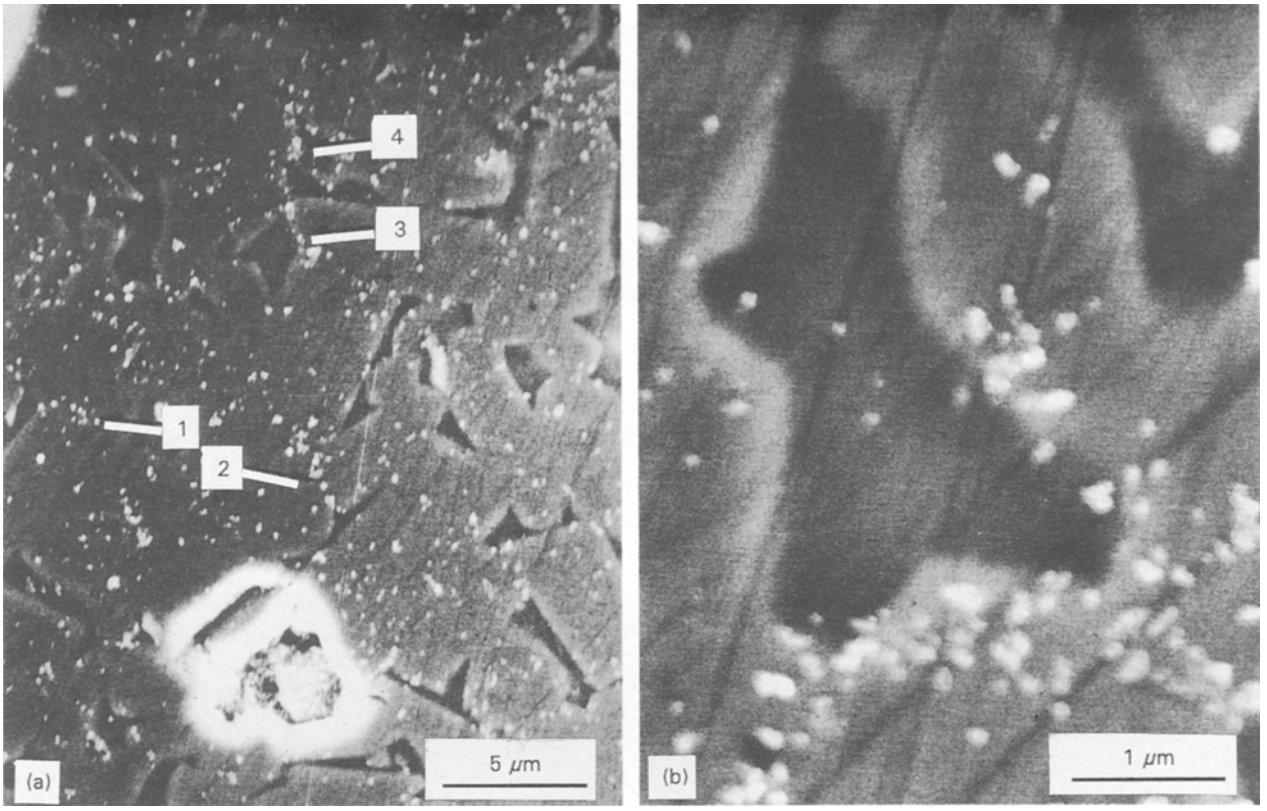

Figure 5 Scanning elecron micrographs of a charged ceramic surface developed by liquid toner.

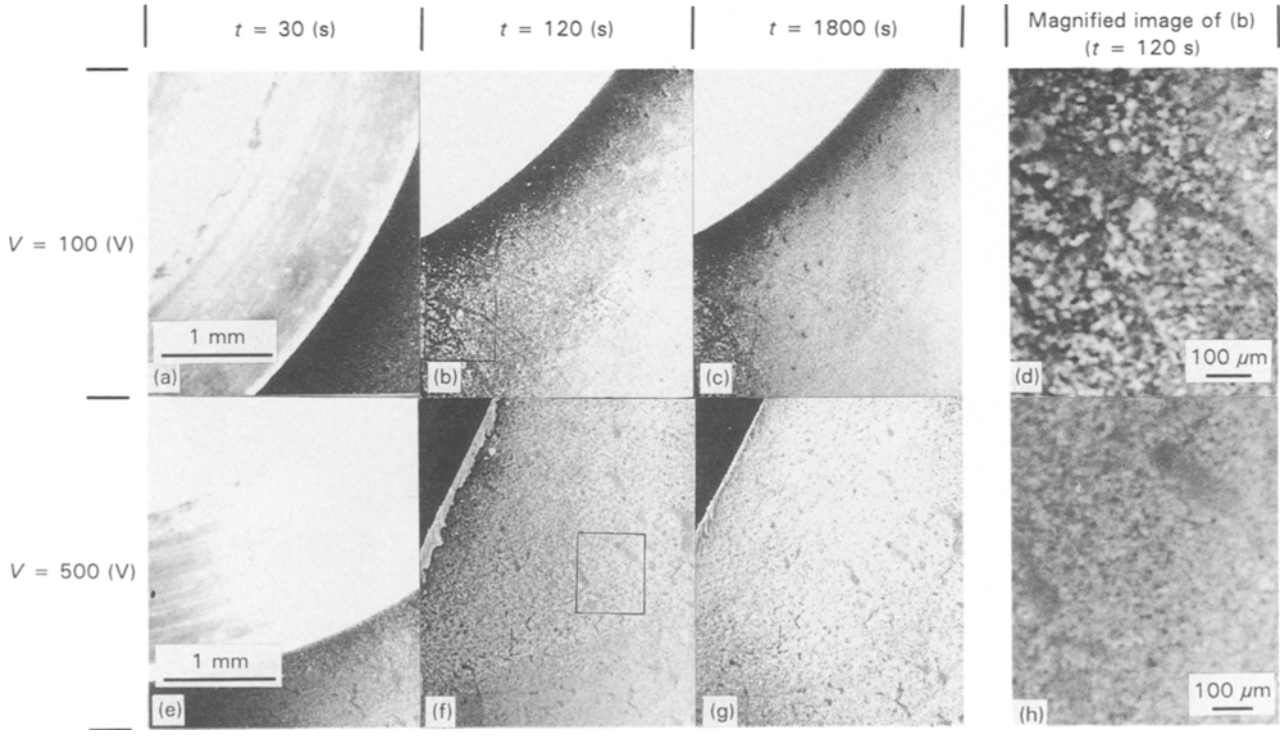

Figure 6 A series of SEM images of charge contrast. (a–c) Applied voltage of 100 V, (e–g) applied voltage of 500 V. (d,h) Enlarged images of (b, f).

phase. Many of these examinations suggest that the granular contrast is mainly located on grain boundaries of the alumina grains or on the interface between the alumina and silicon-rich phase.

3.4. Charge distribution on ceramic electrostatic chuck

The resistivity of alumina sintered in a reducing atmosphere decreases with addition of TiO_2. Therefore,

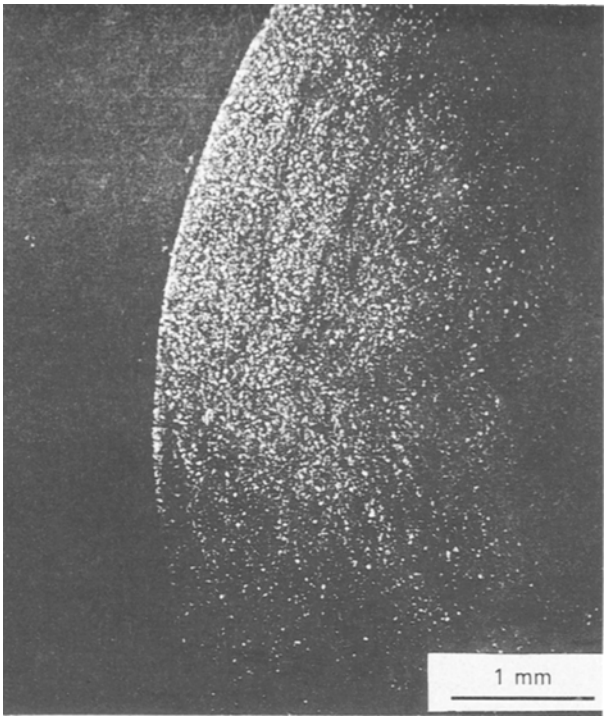

Figure 7 Charge contrast photograph. The image was taken 60 s after removal of the metal plate.

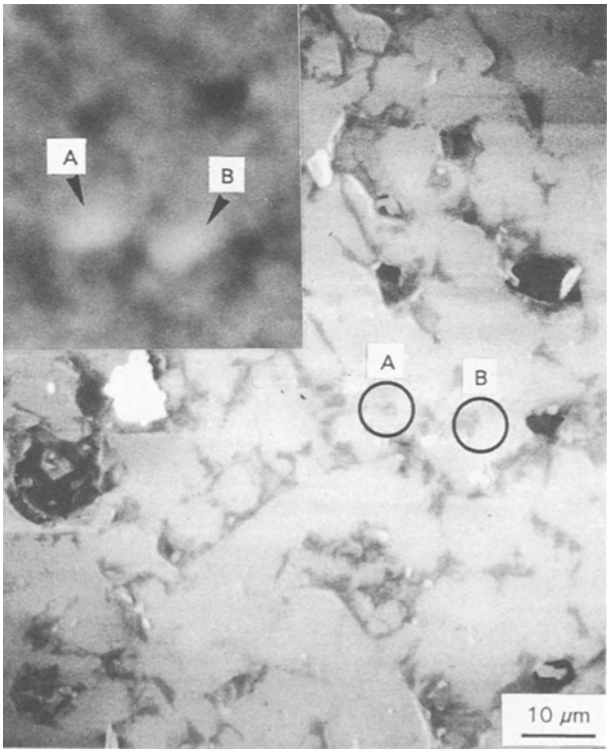

Figure 8 Comparison of the charge contrast image with the microstructural photograph.

TiO_2 particles and neighbouring silicon-rich phase have a lower resistivity than that of alumina grains. When voltage is applied to the electrostatic chuck, charge injected from the inner electrode, first passes through the silicon-rich phase and the TiO_2 particles with low resistance, and then accumulates on the grain boundaries of alumina or on the interfaces between the alumina and silicon-rich phase. Contact conditions are also important factors which affect the charge distribution. Charges are considered to concentrate on higher capacitance and higher insulative contact areas.

Charge trapped on grain boundaries or interfaces lasts even after terminating the voltage application, and this causes the residual electrostatic force. Although we did not obtain a clear distribution image of longer-lasting homocharge, it is considered also to be trapped on the grain boundaries or interfaces. It has been reported that the high-resistance secondary phase is locally charged in the SEM image [18]. Direct charge injection into the deep traps on grain boundaries or interfaces can cause long-lasting homocharge. These homocharges also affect the heterocharge, sometimes stabilizing the heterocharge by forming positive and negative charge pairs. Therefore, residual charge depends on the microstructural uniformity of ceramics, including resistance and permittivity uniformity, as well as the average value of resistance and permittivity.

4. Conclusions

Electrostatic charge and its distribution on TiO_2- and Cr_2O_3-added alumina electrostatic chucks was studied. Electrostatic potential measurements and SEM observation of space charge by two methods were made.

1. Homocharge in addition to heterocharge appears on the ceramics when the applied voltage is above 330 V and the homocharge lasts longer than heterocharge. On the other hand, only homocharge appears on the ceramics when the applied voltage is below 330 V. Homocharge is attributed to corona discharge from the electrode.

2. Heterocharge was observed as granular contrast via SEM observation and the charge is considered to be concentrated mainly on the alumina grain boundaries or interfaces between alumina and the silicon-rich phase.

Acknowledgements

The authors acknowledge helpful discussions with Professor Y. Murata, Science University of Tokyo. The authors also thank Mr T. Aoshima and Mr Y. Aso, Toto Ltd, for their technical assistance with the SEM observation and other experiments.

References

1. T. WATANABE and T. KITABAYASHI, *J. Jpn Ceram. Soc* **100** (1992) 1.
2. T. WATANABE, T. KITABAYASHI and C. NAKAYAMA, *Jpn J. Appl. Phys.* **31** (1992), to be published.
3. T. WATANABE, *Oyo-kikai-kogaku (Appl. Mech. Eng.)* **5** (1989) 128 (in Japanese).
4. F. KANEKO and S. KOBAYASHI, *IEE. Jpn Trans.* **105-A** (1985) 19 (in Japanese).
5. Y. SUZUKI, H. MUTO, T. MIZUTANI and M. IEDA, *J. Phys. D Appl. Phys.* **18** (1985) 2293.

6. P. K. C. PILLAI, G. K. NARULA, A. K. TRIPATHI and R. G. MENDIRATTA, *Phys. Status Solidi* **A77** (1983) 693.
7. A. Y. KO and J. HIRSCH, *Solid State Commun.* **39** (1981) 215.
8. K. OKAZAKI and K. NAGATA, *J. Am. Ceram. Soc.* **56** (1973) 83.
9. C. ALEMANY, B. JIMENEZ, J. MENDIOLA and E. MAURER, *J. Mater. Sci.* **19** (1984) 2555.
10. J. LEWINER, in "Proceedings of the 5th International Symposium on Electrets", Heidelberg (IEE; NY, 1985) p. 202.
11. C. ZHONGYANG and Y. XI, *Ferroelectrics* **109** (1990) 155.
12. S. B. LANG, *ibid.* **74** (1987) 357.
13. D. K. DAS-GUPTA and K. DOUGHTY, IEE Conference Publication No. 239 (1984) p. 164.
14. K. SATO, J. TANAKA, H. HANEDA, A. WATANABE and S. SHIRASAKI, *J. Jpn. Ceram. Soc.* **97** (1989) 1228.
15. K. TUDA and K. MUKAE, *ibid.* **97** (1989) 1211.
16. T. MAEDA and M. TAKATA, *ibid.* **97** (1989) 1219.
17. K. A. METCALFE, *J. Sci. Instrum.* **32** (1955) 74.
18. H. NEMOTO, *J. Am. Ceram. Soc.* **74** (1991) 1719.

Received 15 June 1992
and accepted 20 August 1993